frontiers | Frontiers in Physics

TYPE Original Research
PUBLISHED 23 February 2023
DOI 10.3389/fphy.2023.978347

OPEN ACCESS

EDITED BY
Carlo Gabbanini,
CNR INO, Italy

REVIEWED BY
C. O. Edet,
Cross River University of Technology, Nigeria
Boumali Abdelmalek,
University of Tébessa, Algeria

*CORRESPONDENCE
E. S. Eyube,
edwineyubes@mau.edu.ng

SPECIALTY SECTION
This article was submitted to Atomic and Molecular Physics, a section of the journal Frontiers in Physics

RECEIVED 25 June 2022
ACCEPTED 13 February 2023
PUBLISHED 23 February 2023

CITATION
Eyube ES, Notani PP, Nyam GG, Jabil YY and Izam MM (2023), Pure vibrational state energies and statistical-mechanical models for the reparameterized scarf oscillator.
Front. Phys. 11:978347.
doi: 10.3389/fphy.2023.978347

Pure vibrational state energies and statistical-mechanical models for the reparameterized scarf oscillator

E. S. Eyube[1]*, P. P. Notani[2], G. G. Nyam[3], Y. Y. Jabil[4] and M. M. Izam[4]

[1]Department of Physics, Faculty of Physical Sciences, Modibbo Adama UniversityYola, Adamawa, Nigeria, [2]Department of Pure and Applied Sciences, Taraba State PolytechnicJalingo, Taraba, Nigeria, [3]Department of Physics, Faculty of Science, University of AbujaAbuja, Nigeria, [4]Department of Physics, Faculty of Natural Sciences, University of JosJos, Plateau, Nigeria

In this work, the reparameterized Scarf II oscillator was employed to describe the internal vibration of diatomic systems. Analytical equations for bound state pure vibrational energies and canonical partition function were obtained. The equations were used to derive statistical-mechanical models for the prediction of molar entropy, enthalpy, Gibbs free energy and constant pressure (isobaric) heat capacity of gaseous substances. The obtained model equations were used to generate numerical data on bound state energy eigenvalues and, to investigate the thermodynamic properties of the ground states chloroborane (BCl), bromine fluoride (BrF), and bromine chloride (BrCl) molecules. With the aid of the expression for molar entropy of the system, average absolute deviations obtained for the molecules are 0.1878%, 0.1267%, and 0.0586% from experimental data. The isobaric heat capacity model yields average absolute deviation of 2.1608%, 1.8601%, and 1.9805%. The results obtained are in good agreement with available literature data on gaseous molecule. The work could be applicable in the fields of molecular physics, chemical physics, solid-state physics and chemical engineering.

KEYWORDS

schrödinger equation, diatomic molecules, energy eigenvalues, entropy, enthalpy, gibbs free energy, specific heat capacity, statistical-mechanical models

1 Introduction

Potential energy function (simply known as potential) is a mathematical model used to describe the interaction of a physical system with its environment. One of the problems of this representation is the absence of a universal potential energy function that can model every atomic and molecular interactions. Numerous versions of potential models have been proposed by chemist and physicist to account for observed atomic and molecular phenomena. The list of potential models includes the Morse potential [1], Eckart potential [2], Frost-Musulin potential [3], Rosen-Morse potential [4], Tietz potential [5], Hua potential [6], and Schiöberg potential [7] amongst others.

A potential energy function whose potential parameters are formulated in terms of the spectroscopic constants of a diatomic molecule is referred to as oscillator. The oscillator is a specialized model potential used to describe interactions in diatomic molecules. A diatomic molecule oscillator is required to satisfy the so-called Varshni conditions [8, 9]. The Varshni

conditions ensure that the potential parameters of an oscillator are expressed in terms of molecular constants such as equilibrium harmonic vibrational frequency (ω_e), rotational-vibrational coupling coefficient (α_e), equilibrium dissociation energy (D_e), anharmonicity constant ($\omega_e x_e$), and equilibrium bond length (r_e) [10].

The solution of Schrödinger and other wave equations of quantum mechanics can be obtained analytically or by numerical approach. Quite a number of analytical solution methods have been suggested in the literature, the Nikiforov-Uvarov (NU) method, exact and proper quantization rules, supersymmetric quantum mechanics approach (SUSYQM), asymptotic iteration method (AIM), and the recently introduced Nikiforov-Uvarov functional analysis (NUFA) method are some of the methods. Some illustrative examples where the different solution techniques are used to solve the Schrödinger equation can be found in Ref. [11–16] and the references therein. The solution of Schrödinger wave equation has been instrumental in retrieving information regarding the quantum mechanical system of interest. For instance, expectation values, information theoretic, optical, magnetic, electrical, and thermodynamic properties of substances have been investigated through eigen energy levels and eigenfunctions of wave Eqs 17–34.

The need to obtain analytical (or statistical-mechanical) models for the prediction of thermodynamic properties of gaseous substances have recently attracted much attention from the research community. The thermodynamic property of a gaseous molecule can be predicted theoretically with the aid of analytical model equation; it can also be determined by experimental procedures. The statistical-mechanical models are easy to use and are not expensive, only few molecular constants of a diatomic molecule are required to predict the thermal property of the system. In contrast, experimental method is time consuming, usually very expensive and require huge experimental task.

Different oscillator models have been employed to describe the internal vibration of diatomic molecules. Through such representation, canonical partition function is obtained which is then used to derive other useful thermodynamic models for the gaseous substance. Statistical-mechanical models such as Helmholtz free energy (F), mean thermal energy (U), entropy (S), enthalpy (H), Gibbs free energy (G), isobaric heat capacity (C_p), and constant volume heat capacity (C_V) have successfully been used to examine thermal properties of substances [35–39].

This paper is concerned with improved versions of hyperbolical-type oscillators. Available three parameter models are the specialized Pöschl-Teller potential [40], improved generalized Pöschl-Teller potential [41], and improved Scarf II potential energy function (ISPEF) [42]. On the other hand, existing four parameter models are the improved Pöschl-Teller potential [43], improved q-deformed Scarf II oscillator [10], and modified hyperbolical-type potential [44]. Analytical expressions for the prediction of molar entropy, enthalpy, Gibbs free energy, and isobaric heat capacity have been obtained with various formulations of the improved hyperbolical-type oscillators [10, 45–48]. However, the reparameterized Scarf oscillator has not been considered in the literature. It is against this background that this research is aimed at obtaining the pure vibrational state energies and some statistical-mechanical models for the reparameterized Scarf oscillator (RSO). The paper is organized as follows. In Section 2, potential parameters are developed for the RSO. Equation for pure vibrational state energy is obtained in Section 3. Statistical-mechanical models are derived in Section 4. Results of numerical computations are discussed in Section 5. A brief conclusion of the work is given in Section 6.

2 Potential parameters of the RSO

In previous study, the Varshni conditions for diatomic molecule potential were used to construct the IqSO. By employing the IqSO, analytical equations for the prediction of molar entropy and Gibbs free energy were derived [10]. However, statistical-mechanical models for the prediction of molar enthalpy and heat capacity have not been reported for the IqSO. In the present work, statistical-mechanical models for the prediction of molar entropy, enthalpy, Gibbs free energy and isobaric heat capacity are obtained using the RSO. The RSO can be obtained by subjecting the ISPEF through the transformation $r \rightarrow r{-}r_0$, where r_0 is a real constant. Using this transformation on Eq. 1 of Ref. [42], the RSO is proposed *via* the following equation

$$V(r) = D_e - \frac{V_1 + V_2 \sinh \alpha (r - r_0)}{\cos \mathrm{h}^2 \alpha (r - r_0)}, \tag{1}$$

where V_1, V_2, and α are the potential parameters. The potential Eq. 1 is an oscillator if it satisfies the following constraints (Varshni conditions)

$$V(r \rightarrow \infty) - V(r \approx r_e) = D_e, \tag{2}$$

$$f_1 = 0, \tag{3}$$

$$f_2 = \mu (2\pi c \omega_e)^2, \tag{4}$$

$$\alpha_e = -\frac{6 B_e^2}{\omega_e}\left(1 + \frac{r_e f_3}{3 f_2}\right), \tag{5}$$

where $B_e = \hbar/(4\pi c \mu r_e^2)$, $\hbar = h/2\pi$, h being the Planck constant, c represents the speed of light, and f_j ($j = 1, 2, 3, \ldots$) is the *jth* derivative of $V(r)$ at $r = r_e$. Substituting Eq. 1 into Eqs 2–4 yields

$$V_1 = D_e\{1 - \sin \mathrm{h}^2 \alpha (r_e - r_0)\}, \tag{6}$$

$$V_2 = 2D_e \sinh \alpha (r_e - r_0), \tag{7}$$

$$\alpha = \pi c \omega_e \left(\frac{2\mu}{D_e}\right)^{\frac{1}{2}}. \tag{8}$$

To obtain the parameter r_0, we first note that $f_2 = 2\alpha^2 D_e$, and $f_3 = -6\alpha^3 D_e \tanh\alpha (r_e - r_0)$. Inserting these expressions into Eq. 5 gives

$$r_0 = r_e + \frac{1}{2\alpha} \ln \left| \frac{1 - \frac{1}{\alpha r_e} - \frac{\omega_e \alpha_e}{6\alpha B_e^2 r_e}}{1 + \frac{1}{\alpha r_e} + \frac{\omega_e \alpha_e}{6\alpha B_e^2 r_e}} \right|. \tag{9}$$

3 Pure vibrational state energy levels for the RSO

In this section, the analytical equation for bound state vibrational energy levels is derived using the Nikiforov-Uvarov (NU) solution approach. To ensure continuity of the concept, a brief outline of the NU method is outlined.

TABLE 1 Molecular and potential parameters of the diatomic molecules analyzed in this work.

Molecule	Molecular state	Molecular parameter				Potential parameter	
		D_e (eV)	r_e (Å)	ω_e (cm^{-1})	α_e (cm^{-1})	α (Å^{-1})	r_0 (Å)
BCl	$X\ ^1\Sigma^+$	5.3429 [54]	1.7159 [55]	839.12 [55]	0.006463 [54]	1.4244	0.8743
BrF	$X\ ^1\Sigma^+$	2.50 [56]	1.7532 [56]	669.9011 [57]	0.0025953 [57]	2.2481	1.2292
BrCl	$X\ ^1\Sigma^+$	[a]2.2625 [58]	2.1361704 [58]	444.276 [55]	0.0007697 [55]	1.9176	1.5499

[a]2.2625 eV = 18,248 cm^{-1}.

3.1 An overview of the NU solution method

The NU solution approach is one of the most widely used methods of solving a second order differential equation. With the aid of a convenient transformation, the Schrödinger equation can be converted to a hypergeometric-type differential equation of the form [11].

$$R''_{\nu J}(s) + \frac{\tilde{\tau}(s)}{\sigma(s)} R'_{\nu J}(s) + \frac{\tilde{\sigma}(s)}{\sigma^2(s)} R_{\nu J}(s) = 0, \tag{10}$$

where $\sigma(s)$, $\tilde{\sigma}(s)$ are polynomials at most of second-degree, $\tilde{\tau}(s)$ is a first-degree polynomial and $R_{\nu J}(s)$ is a function of the hypergeometric-type. Writing $R_{\nu J}(s) = \psi_{\nu J}(s) y_{\nu J}(s)$, by suitably choosing the function $\psi_{\nu J}(s)$, expression Eq. 10 assumes the following form

$$\sigma(s) y''_{\nu J}(s) + \tau(s) y'_{\nu J}(s) + \lambda y_{\nu J}(s) = 0, \tag{11}$$

where

$$\tau(s) = \tilde{\tau}(s) + 2\pi(s), \tag{12}$$

$\pi(s)$ is a polynomial of degree at most one, it is given by [11].

$$\pi(s) = \frac{\sigma' - \tilde{\tau}}{2} \pm \sqrt{\left(\frac{\sigma' - \tilde{\tau}}{2}\right)^2 - \tilde{\sigma}(s) + k\sigma(s)}, \tag{13}$$

k is obtained by requiring that the quantity under the square root is a perfect square of a first degree polynomial. λ is deduced *via* the expression

$$\lambda = k + \pi'(s). \tag{14}$$

Successively differentiating Eq. 11 ν times ($\nu = 0, 1, 2, \ldots$) leads to quantum condition given as

$$\lambda_\nu = -\nu\tau'(s) - \frac{1}{2}\nu(\nu - 1)\sigma''(s). \tag{15}$$

energy eigenvalues are obtained by equating the expressions Eqs 14, 15.

3.2 Solution of schrödinger equation with the RSO by NU method

The radial Schrödinger equation in the presence of any potential field $V(r)$ is given as

$$\left\{-\frac{\hbar^2}{2\mu}\frac{d^2}{dr^2} + V(r) + \frac{J(J+1)}{2\mu r^2}\right\} R_{\nu J}(r) = E_{\nu J} R_{\nu J}(r), \tag{16}$$

where ν, and J are the vibrational and rotational quantum numbers, respectively. $E_{\nu J}$ is the ro-vibrational energy eigenvalue of the quantum state νJ, $R_{\nu J}$ is the corresponding radial wave function. For non-zero values of J, only approximate analytical solutions of Eq. 16 are possible with the RSO. Nevertheless, exact analytical solutions are feasible if $J = 0$, the solutions are referred to as the pure vibrational state solutions. Thus, substituting Eq. 1 into Eq. 16 and letting $J = 0$ gives

$$\frac{d^2R_\nu}{dr^2} + \frac{2\mu}{\hbar^2}\left\{E_\nu - D_e + \frac{V_1 + V_2\sinh\alpha(r - r_0)}{\cosh^2\alpha(r - r_0)}\right\} R_\nu = 0, \tag{17}$$

where $E_{\nu 0} \to E_\nu$, $R_{\nu 0} \to R_\nu$. The substitution $s = \sinh\alpha(r - r_0)$ transforms Eq. 17 to

$$R''_\nu(s) + \frac{s}{1 + s^2} R'_\nu(s) + \frac{-\gamma_\nu s^2 + \gamma_0 s - \gamma_1}{(1 + s^2)^2} R_\nu(s) = 0, \tag{18}$$

where, for compactness the following notations have been used; $\gamma_\nu = -\frac{2\mu}{\alpha^2\hbar^2}(E_\nu - D_e)$, $\gamma_0 = \frac{2\mu V_2}{\alpha^2\hbar^2}$, $\gamma_1 = \gamma_\nu - \frac{2\mu V_1}{\alpha^2\hbar^2}$. Comparing Eqs 10, 18 yields $\tilde{\tau} = s$, $\sigma = 1 + s^2$, $\tilde{\sigma} = -\gamma_\nu s^2 + \gamma_0 s - \gamma_1$. Substituting these expressions in Eq. 13 gives

$$\pi(s) = \frac{1}{2}s \pm \sqrt{\left(k + \gamma_\nu + \frac{1}{4}\right)s^2 - \gamma_0 s + k + \gamma_1}. \tag{19}$$

Setting the discriminant of the expression under square root to zero gives

$$\gamma_0^2 = 4\left(k + \gamma_\nu + \frac{1}{4}\right)(k + \gamma_1). \tag{20}$$

Eq. 20 leads to

$$k = -\frac{1}{2}\left(\gamma_\nu + \gamma_1 + \frac{1}{4}\right) \pm \frac{1}{2}\sqrt{\left(\gamma_\nu - \gamma_1 + \frac{1}{4}\right)^2 + \gamma_0^2}. \tag{21}$$

Thus, k is a two-valued parameter viz: $k = k_-$ obtained by choosing the negative square root, and $k = k_+$ if the positive square root is chosen. Using Eq. 20 to eliminate γ_0 in Eq. 19, with some algebraic simplifications, one obtains

$$\pi(s) = \frac{1}{2}s \pm \left(\sqrt{k + \gamma_\nu + \frac{1}{4}}\, s \pm \sqrt{k + \gamma_1}\right). \tag{22}$$

It is evident that for each value of k, $\pi(s)$ has four possible expressions: π_{--}, π_{-+}, π_{+-}, and π_{++} obtained from all possible combinations of the ± signs in Eq. 22. The next task is to deduce

TABLE 2 Potential energies (cm) and bound state pure vibrational state energies (cm^{-1}) as a function of internuclear separation (Å) for the BCl ($X\ ^1\Sigma^+$) molecule.

ν	r [54]		V (cm^{-1})		E_ν (cm^{-1})		ν	r [54]		V (cm^{-1})		E_ν (cm^{-1})	
	r_{min}	r_{max}	V_{min}	V_{max}	[54]	Eq. 28		r_{min}	r_{max}	V_{min}	V_{max}	[54]	Eq. 28
0	1.6472	1.7872	447.033	407.866	416.825	418.228	21	1.3949	2.4088	12,582.599	17,676.846	15,915.836	16,152.605
1	1.6038	1.8473	1,249.641	1,286.214	1,242.629	1,249.181	22	1.3901	2.4322	13,013.619	18,362.203	16,565.828	16,811.994
2	1.5760	1.8920	2006.183	2,184.574	2058.795	2071.965	23	1.3855	2.4556	13,434.562	19,036.136	17,208.451	17,463.213
3	1.5546	1.9303	2,728.393	3,085.652	2,865.485	2,886.579	24	1.3810	2.4789	13,853.843	19,695.385	17,843.762	18,106.263
4	1.5369	1.9650	3,422.744	3,986.378	3,662.852	3,693.023	25	1.3767	2.5021	14,261.431	20,339.727	18,471.813	18,741.143
5	1.5217	1.9972	4,092.038	4,880.114	4,451.046	4,491.297	26	1.3726	2.5253	14,656.395	20,971.713	19,092.652	19,367.853
6	1.5084	2.0278	4,734.848	5,770.831	5,230.211	5,281.402	27	1.3687	2.5485	15,037.844	21,591.101	19,706.323	19,986.393
7	1.4964	2.0570	5,361.872	6,650.488	6,000.485	6,063.337	28	1.3648	2.5717	15,424.912	22,197.705	20,312.868	20,596.764
8	1.4855	2.0852	5,970.984	7,521.222	6,762.002	6,837.102	29	1.3611	2.5950	15,797.334	22,793.920	20,912.324	21,198.965
9	1.4756	2.1125	6,557.497	8,378.889	7,514.889	7,602.698	30	1.3575	2.6182	16,164.561	23,374.539	21,504.723	21,792.996
10	1.4664	2.1392	7,131.421	9,227.458	8,259.269	8,360.124	31	1.3541	2.6415	16,515.803	23,944.519	22,090.097	22,378.857
11	1.4578	2.1653	7,693.449	10,062.716	8,995.259	9,109.380	32	1.3507	2.6649	16,871.340	24,503.679	22,668.473	22,956.549
12	1.4498	2.1909	8,238.706	10,884.497	9,722.971	9,850.466	33	1.3475	2.6883	17,209.891	25,049.567	23,239.874	23,526.071
13	1.4423	2.2161	8,769.755	11,693.326	10,442.521	10,583.382	34	1.3443	2.7118	17,552.253	25,584.485	23,804.320	24,087.423
14	1.4353	2.2410	9,282.926	12,490.225	11,153.982	11,308.129	35	1.3412	2.7354	17,887.553	26,108.347	24,361.829	24,640.606
15	1.4286	2.2656	9,790.097	13,273.396	11,857.480	12,024.706	36	1.3383	2.7591	18,204.462	26,621.090	24,912.416	25,185.619
16	1.4223	2.2899	10,281.373	14,041.377	12,553.096	12,733.114	37	1.3354	2.7829	18,524.505	27,122.679	25,456.090	25,722.462
17	1.4163	2.3140	10,762.312	14,796.114	13,240.918	13,433.351	38	1.3326	2.8068	18,836.488	27,613.100	25,992.862	26,251.135
18	1.4106	2.3379	11,231.077	15,536.586	13,921.028	14,125.419	39	1.3299	2.8309	19,140.096	28,094.330	26,522.735	26,771.639
19	1.4051	2.3617	11,694.426	16,265.009	14,593.503	14,809.318	40	1.3272	2.8551	19,446.421	28,564.318	27,045.713	27,283.973
20	1.3999	2.3853	12,142.518	16,977.613	15,258.416	15,485.046	...	...	...	...	...	...	...

10.3389/fphy.2023.978347

TABLE 3 Potential energies (cm) and bound state pure vibrational state energies (cm^{-1}) as a function of internuclear separation (Å) for the BrF ($X\ ^1\Sigma^+$) molecule.

ν	r [59]		V (cm^{-1})		E_ν (cm^{-1})	
	r_{min}	r_{max}	V_{min}	V_{max}	RKR [59]	Eq. 28
0	1.7046	1.8195	262.9	394.9	334.3	333.1
1	1.6682	1.8683	856.5	1,081.5	996.5	991.9
2	1.6448	1.9043	1,448.0	1735.2	1,651.1	1,639.6
3	1.6266	1.9352	2033.2	2,366.8	2,297.6	2,276.1
4	1.6113	1.9634	2,615.3	2,983.7	2,935.1	2,901.5
5	1.5987	1.9889	3,159.4	3,564.8	3,569.0	3,515.7
6	1.5867	2.0141	3,733.8	4,153.1	4,190.7	4,118.9
7	1.5759	2.0383	4,298.9	4,725.4	4,801.0	4,710.9
8	1.5666	2.0609	4,822.8	5,262.2	5,406.7	5,291.8
9	1.5597	2.0804	5,234.3	5,724.7	6,019.8	5,861.5
10	1.5473	2.1089	6,022.9	6,395.5	6,596.8	6,420.2
11	1.5433	2.1245	6,290.9	6,758.7	7,178.8	6,967.7
12	1.5340	2.1492	6,940.0	7,325.9	7,751.0	7,504.0
13	1.5283	2.1684	7,355.8	7,758.9	8,316.9	8,029.3

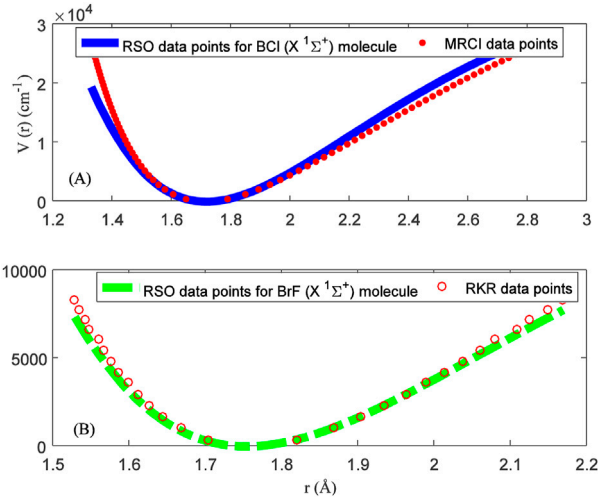

FIGURE 1
Modeling of reparameterized Scarf II oscillator to **(A)** multireference configuration interaction curve for the BCl ($X\ ^1\Sigma^+$) molecule. **(B)** Rydberg-Klein-Rees internuclear potential energy curve for the BrF ($X\ ^1\Sigma^+$).

equations for λ and λ_ν whose results are required to derive vibrational energy levels of the RSO. To satisfy the restriction $\tau'(s) < 0$ of the NU method, we choose from Eqs 21, 22

$$k_+ = -\frac{1}{2}\left(\gamma_\nu + \gamma_1 + \frac{1}{4}\right) + \frac{1}{2}\sqrt{\left(\gamma_\nu - \gamma_1 + \frac{1}{4}\right)^2 + \gamma_0^2}, \tag{23}$$

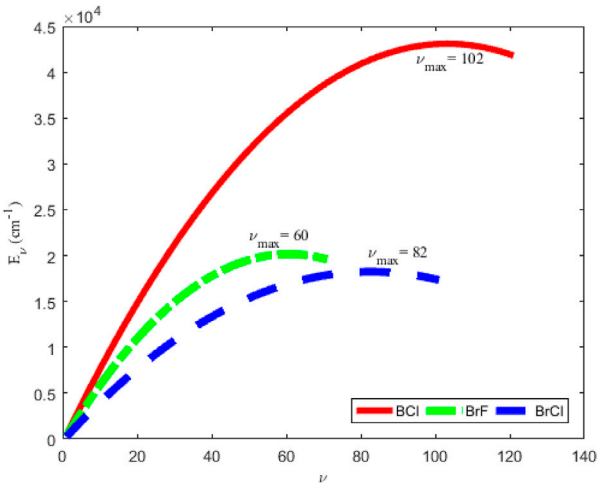

FIGURE 2
Variation of bound state energy eigenvalues *versus* vibrational quantum number for the ground state BCl, BrF, and BrCl molecules.

$$\pi_{--}(s) = \left(\frac{1}{2} - \sqrt{k_- + \gamma_\nu + \frac{1}{4}}\right)s + \sqrt{k_- + \gamma_1}. \tag{24}$$

with the help of expressions Eqs 12, 23, 24, gives

$$\tilde{\tau}(s) = \left(2 - 2\sqrt{k_- + \gamma_\nu + \frac{1}{4}}\right)s + 2\sqrt{k_- + \gamma_1}. \tag{25}$$

with the help of relationships Eqs 23–25, and recalling that $\tilde{\tau}(s) = s, \sigma(s) = 1 + s^2$, Eqs 14, 15 gives

$$\lambda_\nu = -\nu(\nu+1) + 2\nu\sqrt{\frac{1}{2}\left(\gamma_\nu - \gamma_1 + \frac{1}{4}\right) + \frac{1}{2}\sqrt{\left(\gamma_\nu - \gamma_1 + \frac{1}{4}\right)^2 + \gamma_0^2}}, \tag{26}$$

$$\lambda = \frac{3}{8} - \frac{1}{2}(\gamma_\nu + \gamma_1) + \frac{1}{2}\sqrt{\left(\gamma_\nu - \gamma_1 + \frac{1}{4}\right)^2 + \gamma_0^2} - \sqrt{\frac{1}{2}\left(\gamma_\nu - \gamma_1 + \frac{1}{4}\right) + \frac{1}{2}\sqrt{\left(\gamma_\nu - \gamma_1 + \frac{1}{4}\right)^2 + \gamma_0^2}}. \tag{27}$$

By equating expressions Eqs 26, 27, and eliminating γ_ν, γ_0, γ_1 in the resulting equation, the vibrational energy levels for the RSO is obtained as

$$E_\nu = D_e - \frac{\alpha^2\hbar^2}{2\mu}\left\{\nu + \frac{1}{2} - \sqrt{\frac{1}{8} + \frac{\mu V_1}{\alpha^2\hbar^2} + \sqrt{\left(\frac{1}{8} + \frac{\mu V_1}{\alpha^2\hbar^2}\right)^2 + \left(\frac{\mu V_2}{\alpha^2\hbar^2}\right)^2}}\right\}^2. \tag{28}$$

The energy spectrum defined by Eq. 28 increases with increasing ν, the upper bound vibrational quantum number, ν_{max} at which the eigen energies ceases to increase is given by $E'_\nu(\nu_{max}) = 0$, where prime denotes derivative with respect to ν. Inserting Eq. 28 into this equation, we find

TABLE 4 Computed data on molar entropy (J mol^{-1} K^{-1}), reduced enthalpy (kJ mol^{-1}), reduced Gibbs free energy, and isobaric specific heat capacity for the BCl ($X\,^1\Sigma^+$) molecule. $N_p = 60$.

T (K) [60]	Entropy		Enthalpy		– Gibbs free energy		Isobaric specific heat capacity	
	S_{NIST} [60]	S Eq. 40	H_{NIST} [60]	H_{red} Eq. 45	G_{NIST} [60]	G_{red} Eq. 48	C_{pNIST} [60]	C_p Eq. 51
300	213.441	212.994	0.059	0.062	213.245	212.786	31.693	33.746
350	218.394	218.225	1.666	1.760	213.635	213.198	32.572	34.132
400	222.794	222.805	3.314	3.475	214.510	214.119	33.335	34.462
450	226.759	226.881	4.997	5.205	215.654	215.314	33.976	34.748
500	230.367	230.555	6.710	6.949	216.948	216.658	34.510	34.997
...	...	...	...	...	...	...	...	...
2,800	294.016	293.471	92.756	91.729	260.889	260.711	38.385	37.613
2,900	295.364	294.792	96.597	95.492	262.055	261.863	38.433	37.648
3,000	296.668	296.069	100.443	99.259	263.187	262.982	38.480	37.683
3,100	297.930	297.305	104.293	103.029	264.287	264.070	38.527	37.716
3,200	299.154	298.503	108.148	106.802	265.358	265.127	38.572	37.750
...	...	...	...	...	...	...	...	...
5,600	321.001	319.837	201.954	198.394	284.938	284.410	39.581	38.595
5,700	321.702	320.521	205.914	202.259	285.577	285.037	39.621	38.634
5,800	322.391	321.194	209.878	206.128	286.205	285.655	39.662	38.673
5,900	323.070	321.856	213.846	210.001	286.824	286.263	39.702	38.712
6,000	323.737	322.508	217.818	213.879	287.434	286.862	39.742	38.751

$$\nu_{\max} = -\frac{1}{2} + \sqrt{\frac{1}{8} + \frac{\mu V_1}{\alpha^2 \hbar^2} + \sqrt{\left(\frac{1}{8} + \frac{\mu V_1}{\alpha^2 \hbar^2}\right)^2 + \left(\frac{\mu V_2}{\alpha^2 \hbar^2}\right)^2}}. \tag{29}$$

Therefore, ν can assume values 0, 1, 2, ..., $[\nu_{\max}]$. Here, the notation $[\nu_{\max}]$ means the largest integer less than $\nu_{\max}$ for non-integer values of $\nu_{\max}$.

4 Some statistical-mechanical models for the RSO

The partition function is the master key connecting the microscopic model of a system with its macroscopic property. Other thermodynamic quantities can easily be expressed in terms of the partition function. Therefore, explicit expression of the partition function of a gas system is vital in this study. Statistical-mechanical models considered in this paper include molar entropy, enthalpy, Gibbs free energy, and isobaric specific heat capacity.

4.1 The canonical partition function

The canonical partition function of a gaseous molecule is composed of the translation (Q_{tra}), vibrational (Q_{vib}), and rotational (Q_{rot}) [49] components. The canonical partition function is given by the product $Q(T) = Q_{tra}Q_{vib}Q_{rot}$, T being the temperature of the enclosed gas. The vibrational partition function depends on the vibrational energy levels of the diatomic system which in turn depends on the diatomic oscillator used to describe the internal vibration of the gas molecules. The vibrational partition function is given by [50].

$$Q_{vib}(T) = \sum\nolimits_{\nu} g_{\nu} \exp(-\beta E_{\nu}). \tag{30}$$

where g_ν is the factor of the degeneration of the spectrum, $\beta = (k_B T)^{-1}$, k_B is the Boltzmann constant. Given a non-degenerate system of gas molecules, $g_\nu = 1$. Eqs 28–30 leads to

$$Q_{vib}(T) = \exp(-\beta D_e) \sum_{\nu=0}^{\nu_{\max}} \Omega(\nu), \tag{31}$$

where

$$\Omega(\nu) = \exp\left\{\frac{\alpha^2 \beta \hbar^2}{2\mu}(\nu - \nu_{\max})^2\right\}, \tag{32}$$

for a finite series with an upper bound $\nu_{\max}$, the Poisson series formula can be written [51].

$$\sum_{\nu=0}^{\nu_{\max}} \Omega(\nu) = \frac{1}{2}\{\Omega(0) - \Omega(\nu_{\max} + 1)\} + \sum_{j=-\infty}^{j=+\infty} \times \int_0^{\nu_{\max}+1} \Omega(y) \exp(-i(2\pi j y))\mathrm{d}y, \tag{33}$$

TABLE 5 Computed data on molar entropy (J mol^{-1} K^{-1}), reduced enthalpy (kJ mol^{-1}), reduced Gibbs free energy, and isobaric specific heat capacity for the BrF (X $^1\Sigma^+$) molecule. N_p = 60.

T(K) [60]	Entropy		Enthalpy		– Gibbs free energy		Isobaric specific heat capacity	
	S_{NIST} [60]	S Eq. 40	H_{NIST} [60]	H_{red} Eq. 45	G_{NIST} [60]	G_{red} Eq. 48	C_{pNIST} [60]	C_p Eq. 51
300	229.171	228.945	0.061	0.064	228.968	228.733	32.991	34.346
350	234.324	234.269	1.733	1.791	229.373	229.153	33.852	34.730
400	238.891	238.928	3.443	3.536	230.283	230.089	34.537	35.054
450	242.991	243.073	5.184	5.295	231.471	231.306	35.080	35.329
500	246.710	246.808	6.949	7.068	232.812	232.673	35.513	35.566
…	…	…	…	…	…	…	…	…
2,800	311.252	310.729	94.040	93.312	277.666	277.403	38.828	38.638
2,900	312.615	312.089	97.925	97.186	278.848	278.576	38.887	38.725
3,000	313.934	313.406	101.817	101.071	279.995	279.715	38.946	38.810
3,100	315.212	314.683	105.714	104.966	281.111	280.823	39.003	38.891
3,200	316.452	315.923	109.618	108.872	282.196	281.900	39.061	38.967
…	…	…	…	…	…	…	…	…
5,600	338.650	338.182	204.967	204.423	302.049	301.678	40.385	37.775
5,700	339.365	338.886	209.008	208.401	302.697	302.324	40.439	37.606
5,800	340.069	339.576	213.055	212.372	303.336	302.961	40.494	37.432
5,900	340.762	340.254	217.107	216.336	303.964	303.587	40.548	37.252
6,000	341.444	340.919	221.164	220.293	304.583	304.204	40.602	37.068

Inserting expression Eq. 32 in Eq. 33 gives

$$\sum_{\nu=0}^{\nu_{\max}}\Omega(\nu)=\frac{1}{2}\left\{\exp\left(\frac{\alpha^2\beta\hbar^2}{2\mu}\right)-\exp\left(\frac{\alpha^2\beta\nu_{\max}^2\hbar^2}{2\mu}\right)\right\}+\sum_{j=-\infty}^{j=+\infty}\exp\left(\frac{2\pi^2\mu j^2}{\alpha^2\beta\hbar^2}-\mathrm{i}2\pi\nu_{\max}j\right)\int_0^{\nu_{\max}+1}\exp\left\{\frac{\alpha^2\beta\hbar^2}{2\mu}\left(y-\nu_{\max}-\frac{\mathrm{i}2\pi\mu j}{\alpha^2\beta\hbar^2}\right)^2\right\}\mathrm{d}\,y \quad (34)$$

by evaluating the definite integral, Eq. 34 yields

$$\sum_{\nu=0}^{\nu_{\max}}\Omega(\nu)=\frac{1}{2}\left\{\exp\left(\frac{\alpha^2\beta\hbar^2}{2\mu}\right)-\exp\left(\frac{\alpha^2\beta\nu_{\max}^2\hbar^2}{2\mu}\right)\right\}+\sum_{j=-\infty}^{j=+\infty}\frac{1}{\alpha\hbar}\sqrt{\frac{\pi\mu}{2\beta}}\exp\left(\frac{2\pi^2\mu\nu_{\max}^2j^2}{\alpha^2\beta\hbar^2}-\mathrm{i}2\pi\nu_{\max}j\right)\left\{\mathrm{erfi}\left(\alpha\hbar\sqrt{\frac{\beta}{2\mu}}-\frac{\mathrm{i}2\pi\mu j}{\alpha\beta\hbar}\sqrt{\frac{\beta}{2\mu}}\right)+\mathrm{erfi}\left(\alpha\hbar\nu_{\max}\sqrt{\frac{\beta}{2\mu}}+\frac{\mathrm{i}2\pi\mu j}{\alpha\beta\hbar}\sqrt{\frac{\beta}{2\mu}}\right)\right\} \quad (35)$$

where $\mathrm{erfi}(x)=\frac{2}{\sqrt{\pi}}\int_0^x\exp(t^2)\mathrm{d}\,t$ is the imaginary error function of parameter x. Eq. 35 contains quantum correction terms, these are terms with $j\neq 0$, contributions from these terms are significant if T is small. However, if T is large, the contributions from the quantum correction terms are relatively small. The lowest order approximation has previously been used to obtain approximate expression for the high temperature vibrational partition function of diatomic molecule oscillators [52, 53]. In the lowest order approximation, only contribution from the term with j = 0 is considered, the contributions from quantum correction terms are ignored. Due to the temperature range of the diatomic systems considered in this work, with the help of the lowest order approximation model, expression Eq. 35 is reduced to

$$\sum_{\nu=0}^{\nu_{\max}}\Omega(\nu)=\frac{1}{2}\left\{\exp\left(\frac{\alpha^2\beta\hbar^2}{2\mu}\right)-\exp\left(\frac{\alpha^2\beta\nu_{\max}^2\hbar^2}{2\mu}\right)\right\}+\frac{1}{\alpha\hbar}\sqrt{\frac{\pi\mu}{2\beta}}\left\{\mathrm{erfi}\left(\alpha\hbar\sqrt{\frac{\beta}{2\mu}}\right)+\mathrm{erfi}\left(\alpha\hbar\nu_{\max}\sqrt{\frac{\beta}{2\mu}}\right)\right\}. \quad (36)$$

If the molecules of a diatomic gas are visualized as rigid rotors, neglecting molecular interactions, the translational and rotational partition functions are given as [33, 47].

$$Q_{\mathrm{tra}}(T)=\left(\frac{2\pi m\,k_B\,T}{h^2}\right)^{\frac{3}{2}}\frac{k_B\,T}{p}, \quad (37)$$

$$Q_{\mathrm{rot}}(T)=\frac{T}{\sigma\,\Theta_{\mathrm{rot}}}\left\{1+\frac{1}{3}\frac{\Theta_{\mathrm{rot}}}{T}+\frac{1}{15}\left(\frac{\Theta_r}{T}\right)^2+\frac{4}{315}\left(\frac{\Theta_{\mathrm{rot}}}{T}\right)^3\right\}, \quad (38)$$

where σ is assigned the value 1, 2 for heteronuclear and homonuclear diatomic molecules, respectively. $\Theta_{\mathrm{rot}}=\hbar^2/(2\mu r_e^2 k_B)$ is the characteristic temperature, m is the mass of the molecules which make up gas, p is the gas pressure.

TABLE 6 Computed data on molar entropy (J mol^{-1} K^{-1}), reduced enthalpy (kJ mol^{-1}), reduced Gibbs free energy, and isobaric specific heat capacity for the BrCl (X $^1\Sigma^+$) molecule. $N_p = 60$.

T(K) [60]	Entropy		Enthalpy		– Gibbs free energy		Isobaric specific heat capacity	
	S_{NIST} [60]	S Eq. 40	H_{NIST} [60]	H_{red} Eq. 45	G_{NIST} [60]	G_{red} Eq. 48	C_{pNIST} [60]	C_p Eq. 51
300	240.218	240.256	0.065	0.065	240.002	240.038	35.015	35.302
350	245.662	245.724	1.831	1.839	240.430	240.469	35.604	35.638
400	250.445	250.501	3.622	3.628	241.389	241.431	36.029	35.910
450	254.708	254.744	5.432	5.429	242.637	242.679	36.344	36.134
500	258.550	258.561	7.256	7.241	244.039	244.080	36.586	36.322
…	…	…	…	…	…	…	…	…
2,800	323.446	323.235	94.448	94.365	289.714	289.534	38.549	38.948
2,900	324.799	324.608	98.305	98.277	290.901	290.719	38.593	39.027
3,000	326.108	325.938	102.166	102.199	292.053	291.871	38.637	39.099
3,100	327.376	327.227	106.032	106.132	293.172	292.991	38.681	39.162
3,200	328.605	328.479	109.903	110.076	294.260	294.081	38.724	39.215
…	…	…	…	…	…	…	…	…
5,600	350.536	350.785	204.072	205.732	314.095	314.047	39.745	36.704
5,700	351.240	351.481	208.049	209.665	314.740	314.698	39.788	36.488
5,800	351.932	352.163	212.030	213.587	315.375	315.338	39.830	36.270
5,900	352.614	352.832	216.015	217.499	316.001	315.968	39.872	36.049
6,000	353.284	353.488	220.004	221.401	316.617	316.588	39.914	35.826

4.2 Molar entropy model for the RSO

The molar entropy for the system is evaluated from the expression [48].

$$S = R\ln Q + RT\left(\frac{\partial \ln Q}{\partial T}\right)_V, \tag{39}$$

where $R = N_A k_B$ is the molar gas constant, N_A is the Avogadro number, V is the volume of gas enclosed. Substituting $Q = Q_{tra}Q_{vib}Q_{rot}$ into the second term in Eq. 39 gives

$$S = R\left(\ln Q + \Xi_{vib} + \frac{5}{2}\right) + \frac{R}{\sigma Q_{rot}}\left(\frac{T}{\Theta_{rot}} - \frac{1}{15}\frac{\Theta_{rot}}{T} - \frac{8}{315}\frac{\Theta_{rot}^3}{T^3}\right), \tag{40}$$

where, for brevity we have employed the representation

$$\Xi_{vib} = \frac{\beta}{2Q_{vib}}\left\{\begin{array}{l}\left(D_e - \frac{\alpha^2\hbar^2}{2\mu} - \frac{1}{\beta}\right)\exp\left(\frac{\alpha^2\beta\hbar^2}{2\mu}\right) - \left(D_e - \frac{\alpha^2\nu_{max}^2\hbar^2}{2\mu} + \frac{\nu_{max}}{\beta}\right)\exp\left(\frac{\alpha^2\beta\nu_{max}^2\hbar^2}{2\mu}\right) \\ + \frac{\nu_{max}}{\alpha\hbar}\sqrt{\frac{2\pi\mu}{\beta}}\left(D_e + \frac{1}{2\beta}\right)\left[\mathrm{erfi}\left(\alpha\hbar\sqrt{\frac{\beta}{2\mu}}\right) + \mathrm{erfi}\left(\alpha\nu_{max}\hbar\sqrt{\frac{\beta}{2\mu}}\right)\right]\end{array}\right\}\exp(-\beta D_e). \tag{41}$$

4.3 Molar enthalpy model for the RSO

The molar enthalpy of the system is defined by the equation [48].

$$H = RT^2\left(\frac{\partial \ln Q}{\partial T}\right)_V + RTV\left(\frac{\partial \ln Q}{\partial V}\right)_T. \tag{42}$$

with the aid of the substitution $Q = Q_{tra}Q_{vib}Q_{rot}$, expression Eq. 42 and the relations Eqs 36–38 gives

$$H = RT\left\{\Xi_{vib} + \frac{5}{2} + \frac{1}{\sigma Q_{rot}}\left(\frac{T}{\Theta_{rot}} - \frac{1}{15}\frac{\Theta_{rot}}{T} - \frac{8}{315}\frac{\Theta_{rot}^3}{T^3}\right)\right\}. \tag{43}$$

For the purpose of comparing theoretical results to experimental data, the reduced molar enthalpy is considered, it is given as [46–48].

$$H_{red} = H - H'_{298.15} \tag{44}$$

where $H_{298.15}$ is the molar enthalpy computed at $p = 1$ bar, and $T = 298.15$ K. Therefore, putting Eq. 43 in Eq. 44, we have

$$H_{red} = RT\left\{\Xi_{vib} + \frac{5}{2} + \frac{1}{\sigma Q_{rot}}\left(\frac{T}{\Theta_{rot}} - \frac{1}{15}\frac{\Theta_{rot}}{T} - \frac{8}{315}\frac{\Theta_{rot}^3}{T^3}\right)\right\} - H'_{298.15} \tag{45}$$

4.4 Molar Gibbs free energy model for the RSO

The molar Gibbs free energy of the system can be deduced from the expression [48].

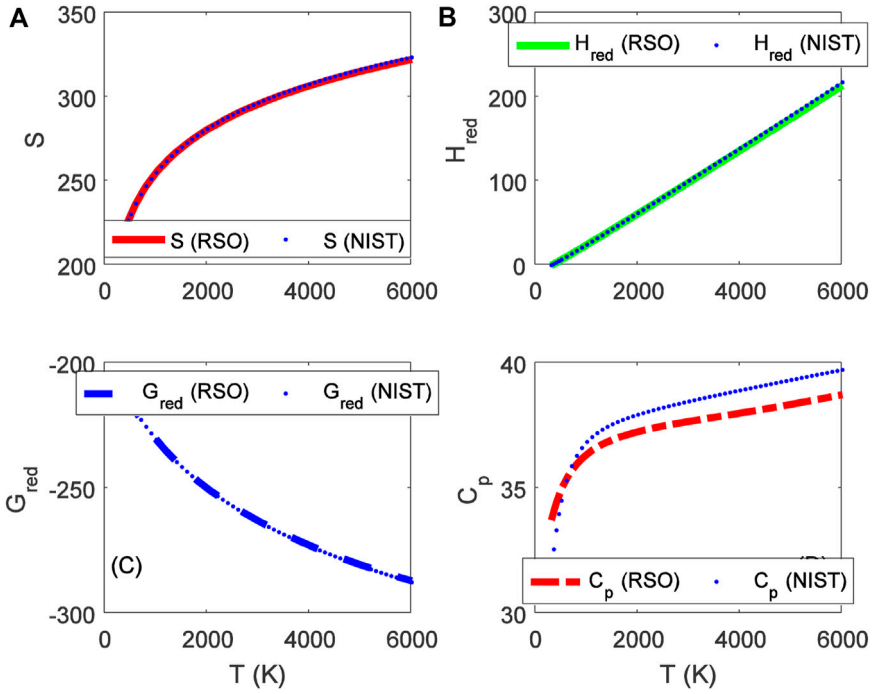

FIGURE 3
Variation of **(A)** molar entropy (J mol^{-1} K^{-1}), **(B)** reduced enthalpy (kJ mol^{-1}), **(C)** reduced Gibbs free energy (J mol^{-1} K^{-1}), and **(D)** isobaric specific heat capacity as a function of temperature for the ground state BCl ($X\ ^1\Sigma^+$) molecule.

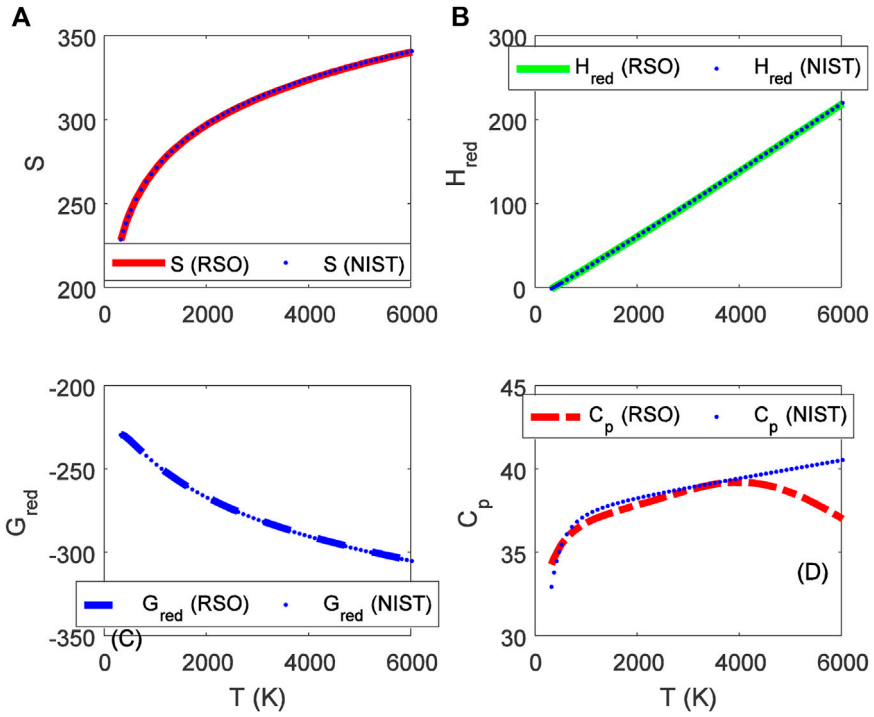

FIGURE 4
Variation of **(A)** molar entropy (J mol^{-1} K^{-1}), **(B)** reduced enthalpy (kJ mol^{-1}), **(C)** reduced Gibbs free energy (J mol^{-1} K^{-1}), and **(D)** isobaric specific heat capacity as a function of temperature for the ground state BrF ($X\ ^1\Sigma^+$) molecule.

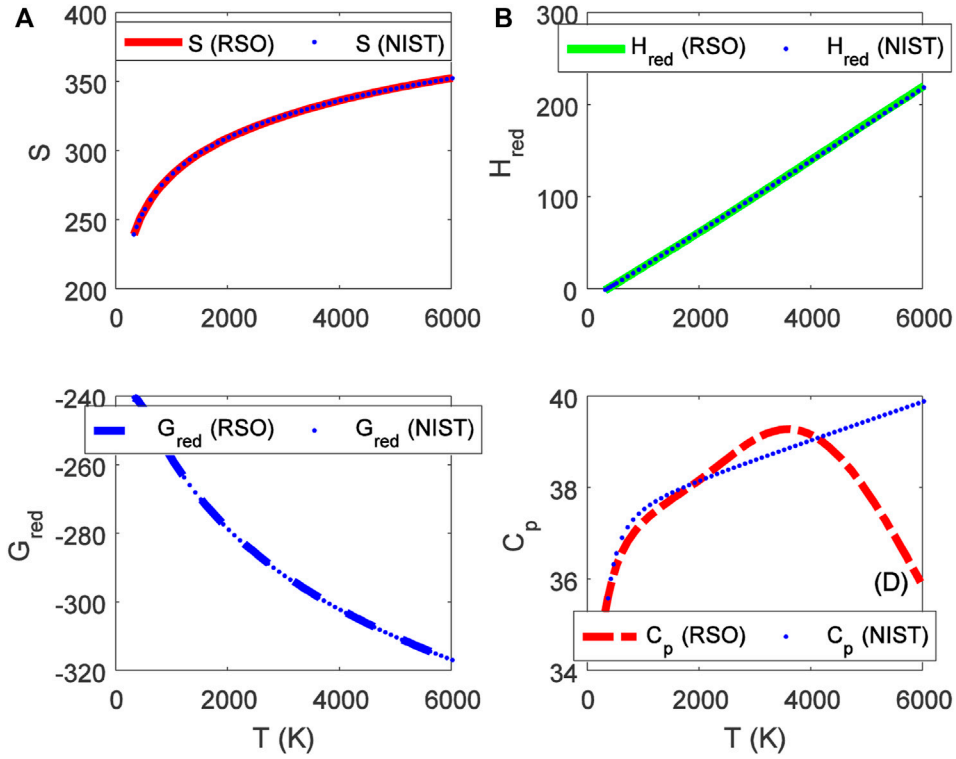

FIGURE 5
Variation of **(A)** molar entropy (J mol^{-1} K^{-1}), **(B)** reduced enthalpy (kJ mol^{-1}), **(C)** reduced Gibbs free energy (J mol^{-1} K^{-1}), and **(D)** isobaric specific heat capacity as a function of temperature for the ground state BrCl ($X\ ^1\Sigma^+$) molecule.

$$G = RTV\left(\frac{\partial \ln Q}{\partial V}\right)_T - RT\ln Q. \tag{46}$$

Inserting the equation of canonical partition function in to the first term of Eq. 46, we obtain the molar Gibbs free energy in compact form as

$$G = -RT\ln Q. \tag{47}$$

The reduced or scaled Gibbs free energy is often required for comparison with experimental data, it is given as $G_{red} = (G-H'_{298.15})/T$. Inserting Eq. 47 into this equation yields

$$G_{red} = -\left(R\ln Q + H'_{298.15}/T\right). \tag{48}$$

4.5 Molar specific heat capacity model for the RSO

Molar specific heat capacity at constant pressure can be deduced from the Eq. 33.

$$C_p = \frac{\partial H}{\partial T}. \tag{49}$$

Substituting Eq. 43 in Eq. 49 and using expressions Eqs 36–38 to simplify the resulting equation, we obtained

$$C_p = R\left(\frac{5}{2} + 2\Xi_{vib} - \Xi_{vib}^2 + \Gamma_{vib}\right) + \frac{2R}{\sigma Q_{rot}}\left(\frac{T}{\Theta_{rot}} + \frac{4}{315}\frac{\Theta_{rot}^2}{T^2}\right) - \frac{R}{\sigma Q_{rot}}\left(\frac{1}{15} + \frac{T^2}{\Theta_{rot}^2} + \frac{16}{315}\frac{\Theta_{rot}}{T}\right)^2, \tag{50}$$

where the parameter Γ_{vib} is given by

$$\Gamma_{vib} = \frac{1}{2Q_{vib}}\left\{\begin{array}{c}\left[\left(\beta D_e - \frac{\alpha^2\hbar^2}{2\mu} - 2\right)^2 - \frac{\alpha^2\hbar^2}{2\mu} - \frac{1}{2}\right]\exp\left(\frac{\alpha^2\beta\hbar^2}{2\mu}\right) \\ -\left[\left(\beta D_e - \frac{\alpha^2\beta\nu_{max}^2\hbar^2}{2\mu} + \nu_{max} - 1\right)^2 + \frac{\alpha^2\beta\nu_{max}^2\hbar^2}{2\mu} - \varepsilon^2 + \frac{3}{2}\nu_{max} - 1\right]\exp\left(\frac{\alpha^2\beta\nu_{max}^2\hbar^2}{2\mu}\right) \\ +\frac{\nu_{max}}{\alpha\hbar}\sqrt{\frac{2\pi\mu}{\beta}}\left(D_e + \frac{1}{2\beta}\right)\left[\left(\beta D_e - \frac{1}{2}\right)^2 - \frac{1}{2}\right]\left[\mathrm{erfi}\left(\alpha\hbar\sqrt{\frac{\beta}{2\mu}}\right) + \mathrm{erfi}\left(\alpha\nu_{max}\hbar\sqrt{\frac{\beta}{2\mu}}\right)\right] \\ \exp\left(-\beta D_e\right).\end{array}\right\} \tag{51}$$

5 Results and discussion

In this section, the analytical equations developed for the reparameterized Scarf II oscillator are analyzed on some selected diatomic molecules. The experimental values of the relevant molecular constants D_e, r_e, ω_e, α_e of the ground state BCl, BrF, and BrCl molecules are taken from Refs. [54–59]. The molecular constants and computed potential parameters of the molecules are shown in Table 1.

With the aid of Eq. 1, potential energy data, $V(r_{min}) = V_{min}$, and $V(r_{max}) = V_{max}$ are obtained. Due to unavailability of literature data on BrCl molecule, only results for BCl and BrF molecules are obtained. Tables 2, 3 summarizes results of numerical computations, and available literature data on vibrational energies of the molecules. The literature data were those obtained by multireference configuration interaction (MRCI), and Rydberg-Klein-Rees (RKR) method [54, 59].

Figure 1 shows graphical fitting of the RSO to (A) MRCI data points of BCl molecule, and (B) RKR data points of BrF molecule. The plots reveal that the RSO could model the internuclear potential energy curves of the BCl and BrF molecules. However, graphical plots only give an idea of the agreement between predicted data and experimental results. The average absolute deviation from experimental data (σ_{ave}) is one of the most widely used goodness-of-fit indicators to evaluate the accuracy of an empirical model. Previously, the average absolute deviation has been used to substantiate the accuracy of proposed model Eqs 38, 41, 43, 48. The average absolute deviation can be written as

$$\sigma_{ave} = \frac{100}{N_p}\sum\left|\frac{X - Y}{Z}\right|. \tag{52}$$

where N_p is the number of experimental data points, (X, Y, Z) ≡ (V, E, S, H, G, C_p). Average absolute deviations less than 1% shows good agreement between predicted and observed data, the smaller the σ_{ave}, better the model.

Using Eq. 52 and the data in Tables 2, 3, average absolute deviations of 5.3976% and 1.6790% are obtained from the experimental data of the BCl and BrF molecules, respectively. The results show that data predicted by the RSO are relatively high for the BCl molecule. To within 2% error limit of the RKR data, the RSO can approximately reproduced the internuclear potential energy curve of the ground state BrF molecule.

Figure 2 shows the variation of energy levels Eq. 28 of the molecules against vibrational quantum number, ν. The plot reveal that as ν is gradually increased from zero, the energy of the molecules also increases. The upper bound vibrational quantum numbers obtained for the BCl, BrF and BrCl molecules are 102, 60 and 82, respectively. As ν is further increased beyond ν_{max}, the bound state energy of the molecules begins to decrease, leading to degenerate energy levels of the molecules. Eq. 28 is also used to generate numerical data on bound state pure vibrational energies of the molecules. As there are no available literature data on energies of BrCl molecule to allow comparison, only the results for BCl and BrF molecules are displayed in Tables 2, 3. Using Eq. 52 and the energy data in Tables 2, 3, average absolute deviation obtained are 1.1949% for BCl molecule, and 1.8353% for BrF molecule. Thus, it can be seen that the energy values predicted by expression Eq. 28 are in good agreement with existing experimental data on the diatomic molecules.

To authenticate the applicability of the statistical-mechanical models proposed in this study, Eq. 43 is used to compute the value of $H'_{298.15}$ at $T = 298.15$ K, $p = 0.1$ MPa to yield; 14.502 kJmol^{-1} for BCl, 13.626 kJmol^{-1} for BrF and 12.533 kJmol^{-1} for BrCl molecules. Using these results and the data in Table 1, the expressions for molar entropy Eq. 40, reduced enthalpy Eq. 45, reduced Gibbs free energy Eq. 48, and constant pressure specific heat capacity Eq. 51 are used to obtain numerical data for the diatomic molecules. The computations are carried out at $p = 0.1$ MPa and temperature in the range 300 K–6,000 K. The results of computations are shown in Tables 4–6. Also included in the tables are literature data on molar entropy (S_{NIST}), reduced molar enthalpy (H_{NIST}), reduced molar Gibbs free energy (G_{NIST}) and constant pressure specific heat capacity (C_{pNIST}). The data are those reported in the National Institute of Standards and Technology (NIST) database [60]. Figures 2–5 represent the temperature variation of the thermal functions.

Choosing X ≡ Z ≡ S_{NIST} to represent experimental data on molar entropy and setting Y ≡ S, average absolute deviations obtained for the BCl, BrF and BrCl molecules are 0.2011%, 0.1224% and 0.5323%, respectively. Thus, it is obvious that within error limit of 1% of the NIST data, entropy equation proposed in this work can accurately predict the experimental data on molar entropy of the diatomic molecules.

To confirm the suitability of expression Eq. 45 to predict molar entropy of the diatomic molecules, we let X ≡ Y ≡ H_{NIST} to denote the experimental data on reduced molar entropy. Choosing Y ≡ H_{red}. The average absolute deviation deduced for the diatomic molecules are 1.5346% for BCl, 0.688% for BrF and 0.5323% for BrCl molecules. The results reveal that statistical-mechanical model proposed for the RSO can accurately predict the NIST data on molar enthalpy of the examined molecules.

To show the relevance of expression Eq. 51 to model experimental data on molar Gibbs free energy, average absolute deviation is computed for each of the molecules. By appropriately choosing the parameters in Eq. 52 with respect to experimental data, such that X ≡ Y ≡ G_{NIST}, and Z ≡ G_{red}, average absolute deviations obtained for the BCl, BrF and BrCl diatomic molecules are 0.1033%, 0.0903%, and 0.0367%, respectively. The results show that on a scale of 1% of the NIST data, Gibbs free energy expression proposed by the RSO is a near perfect model to accurately predict experimental results of the examined diatomic molecules.

The analytical expression of constant pressure specific heat capacity is also analyzed for the diatomic molecules. Average absolute deviation deduced for the BCl, BrF, and BrCl molecules are 2.1565%, 1.9731%, and 1.9805%, respectively. The results are in good agreement with NIST data particularly in the low to moderate temperature regions. However, in the high temperature regime, the predicted results are relatively higher than observed data. The discrepancy arises as a result of rigid-rotor approximation of the diatomic molecules and also, the quantum correction terms excluded in the expression of vibrational partition function, which by extension are also excluded in all the statistical-mechanical models of the system.

6 Conclusion

In this paper, conditions to be satisfied by a diatomic molecule potential are used to construct the reparameterized Scarf II oscillator (RSO), suitable for application to diatomic molecules. Using the Nikiforov-Uvarov method to solve the radial Schrödinger equation for the RSO, analytical expression of bound state pure vibrational energy is derived for the system. With the aid of the formula for energy eigenvalues, analytical equations representing canonical partition function and other relevant statistical-mechanical models are obtained, including molar entropy, enthalpy, Gibbs

free energy and isobaric specific heat capacity. The obtained equations were used to study thermodynamic properties of three diatomic molecules *viz* BCl, BrF, and BrCl. Average absolute deviations of 1.5364%, 0.688%, and 0.5323%, respectively are obtained using the expression of reduced molar enthalpy. The equation of reduced Gibbs free energy yields average absolute deviations of 0.1033%, 0.0903%, and 0.0367% for the diatomic molecules. The results are in excellent agreement with existing literature data on the diatomic molecules. The developed statistical-mechanical models could be useful in scientific and engineering researches involving thermochemical processes.

Data availability statement

The original contributions presented in the study are included in the article/Supplementary Material, further inquiries can be directed to the corresponding author.

Author contributions

EE: Conceptualization, methodology, validation, data curation, formal analysis, project administration, supervision, writing–original draft, writing–review and editing. PN: Methodology, formal analysis, validation, data curation, writing–review and editing, formal analysis. GN: Formal analysis, validation, data curation, formal analysis, writing–review and editing. YJ: Methodology, validation, data curation, visualization, supervision, writing–review and editing. MI: Methodology, validation, formal analysis, data curation, visualization, supervision, writing–review and editing.

Conflict of interest

The authors declare that the research was conducted in the absence of any commercial or financial relationships that could be construed as a potential conflict of interest.

Publisher's note

All claims expressed in this article are solely those of the authors and do not necessarily represent those of their affiliated organizations, or those of the publisher, the editors and the reviewers. Any product that may be evaluated in this article, or claim that may be made by its manufacturer, is not guaranteed or endorsed by the publisher.

References

1. Morse PM. Diatomic molecules according to the wave mechanics. II. Vibrational levels. *Phys Rev* (1929) 34:57–64. doi:10.1103/PhysRev.34.57

2. Eckart C. The penetration of a potential barrier by electrons. *Phys Rev* (1930) 35: 1303–9. doi:10.1103/PhysRev.35.1303

3. Frost AA, Musulin B. Semi empirical potential energy functions. I. The H_2 and H_2^+ diatomic molecules. *J Chem Phys* (1954) 22:1017–20. doi:10.1063/1.1740254

4. Rosen N, Morse PM. On the vibrations of polyatomic molecules. *Phys Rev* (1932) 42:210–7. doi:10.1103/PhysRev.42.210

5. Tietz T. Potential-energy function for diatomic molecules. *J Chem Phys* (1963) 38: 3036–7. doi:10.1063/1.1733648

6. Hua W. Four-parameter exactly solvable potential for diatomic molecules. *Phys Rev A* (1990) 42:2524–9. doi:10.1103/PhysRevA.42.2524

7. Schiöberg D. The energy eigenvalues of hyperbolical potential functions. *Mol Phys* (1986) 59:1123–37. doi:10.1080/00268978600102631

8. Yanar H, Aydoğdu O, Saltı M. Modelling of diatomic molecules. *Mol Phys* (2016) 114:3134–42. doi:10.1080/00268976.2016.1220645

9. Horchani R, Al-Kindi N, Jelassi H. Ro-vibrational energies of caesium molecules with the Tietz-Hua oscillator. *Mol Phys* (2020) 119:e1812746. doi:10.1080/00268976.2020.1812746

10. Eyube ES, Nyam GG, Notani PP. Improved q-deformed Scarf II oscillator. *Phys Scr* (2021) 96:125017. doi:10.1088/1402-4896/ac2eff

11. Nikiforov AF, Uvarov VB. *Special functions of mathematical physics*. Basel: Birkhauser (1988). doi:10.1007/978-1-4757-1595-8

12. Horchani R, Al-Aamri H, Al-Kindi S, Ikot AN, Okorie US, Rampho GJ, et al. Energy spectra and magnetic properties of diatomic molecules in the presence of magnetic and AB fields with the inversely quadratic Yukawa potential. *Eur Phys J D* (2021) 75:36. doi:10.1140/epjd/s10053-021-00038-2

13. Ma ZQ, Xu BW. Quantum correction in exact quantization rules. *EPL* (2005) 69: 685–91. doi:10.1209/epl/i2004-10418-8

14. Kumar PR, Dong SH. A new quantization rule to the bound state problem in non-relativistic quantum mechanics. *Phys Lett A* (2021) 417:127700. doi:10.1016/j.physleta.2021.127700

15. Sun GH, Dong Q, Bezetta VB, Dong SH. Exact solutions of an asymmetric double well potential. *J Math Chem* (2022) 60:605–12. doi:10.1007/s10910-022-01328-9

16. Edet CO, Mahmoud S, Inyang PE, Ali N, Aljunid SA, Endut R, et al. Non-Relativistic treatment of the 2D electron system interacting via varshni–shukla potential using the asymptotic iteration method. *Mathematics* (2022) 10:2824. doi:10.3390/math10152824

17. Deng M, Jia CS. Prediction of enthalpy for nitrogen gas. *Eur Phys J Plus* (2018) 133:258. doi:10.1140/epjp/i2018-12090-2

18. Jia CS, Wang CW, Zhang LH, Peng XL, Tang HM, Liu JY, et al. Predictions of entropy for diatomic molecules and gaseous substances. *Chem Phys Lett* (2018) 692: 57–60. doi:10.1016/j.cplett.2017.12.013

19. Jiang R, Jia CS, Wang YQ, Peng XL, Zhang LH. Prediction of enthalpy for the gases CO, HCl, and BF. *Chem Phys Lett* (2018) 715:186–9. doi:10.1016/j.cplett.2018.11.044

20. Jia CS, Wang CW, Zhang LH, Peng XL, Tang HM, Zeng R. Enthalpy of gaseous phosphorus dimer. *Chem Eng Sci* (2018) 183:26–9. doi:10.1016/j.ces.2018.03.009

21. Peng XL, Jiang R, Jia CS, Zhang LH, Zhao YL. Gibbs free energy of gaseous phosphorus dimer. *Chem Eng Sci* (2018) 190:122–5. doi:10.1016/j.ces.2018.06.027

22. Wang J, Jia CS, Li CJ, Peng XL, Zhang LH, Liu JY. Thermodynamic properties for carbon dioxide. *ACS Omega* (2019) 4:19193–8. doi:10.1021/acsomega.9b02488

23. Jia CS, Zhang LH, Peng XL, Luo JX, Zhao YL, Liu JY, et al. Prediction of entropy and Gibbs free energy for nitrogen. *Chem Eng Sci* (2019) 202:70–4. doi:10.1016/j.ces.2019.03.033

24. Horchani R, Jelassi H. A four-parameters model for molar entropy calculation of diatomic molecules via shifted Tietz-Wei potential. *Chem Phys Lett* (2020) 753:137583. doi:10.1016/j.cplett.2020.137583

25. Horchani R, Jelassi H. Accurate and general model to predict molar entropy for diatomic molecules. *S Afr J Chem Eng* (2020) 33:103–6. doi:10.1016/j.sajce.2020.07.001

26. Jia CS, Li J, Liu YS, Peng XL, Jia X, Zhang LH, et al. Predictions of thermodynamic properties for hydrogen sulfide. *J Mol Liq* (2020) 315:113751. doi:10.1016/j.molliq.2020.113751

27. Ikot AN, Edet CO, Amadi PO, Okorie US, Rampho GJ, Abdullah HY. Thermodynamic properties of Aharanov–Bohm (AB) and magnetic fields with screened Kratzer potential. *Eur Phys J D* (2020) 74:159. doi:10.1140/epjd/e2020-10084-9

28. Ikot AN, Okorie US, Osonboye G, Amadi PO, Edet CO, Sithole MJ, et al. Superstatistics of Schrödinger equation with pseudo-harmonic potential in external magnetic and Aharanov-Bohm fields. *Heliyon* (2020) 6:e03738. doi:10.1016/j.heliyon.2020.e03738

29. Ikot AN, Rampho GJ, Amadi PO, Sithole MJ, Okorie US, Lekala MI. Shannon entropy and Fisher information-theoretic measures for Mobius square potential. *Eur Phys J Plus* (2020) 135:503. doi:10.1140/epjp/s13360-020-00525-2

30. Horchani R, Al Shafi S, Friha H, Jrlassi H. A straightforward model for molar enthalpy prediction of CsO, CsF, and CsCl molecules via shifted Tietz-Wei potential. *Int J Thermophys* (2021) 42:84. doi:10.1007/s10765-021-02839-4

31. Wang CW, Wang J, Liu YS, Li J, Peng XL, Jia CS, et al. Prediction of the ideal-gas thermodynamic properties for water. *J Mol Liq* (2021) 321:114912. doi:10.1016/j.molliq.2020.114912

32. Oluwadare OJ, Oyewumi KJ, Abiola TO. Thermodynamic properties of some diatomic molecules confined by an harmonic oscillating system. *Indian J Phys* (2022) 96:1921–8. doi:10.1007/s12648-021-02139-5

33. Fan QC, Jian J, Fan XZ, Fu J, Li HD, Ma J, et al. A method for predicting the molar heat capacities of HBr and HCl gases based on the full set of molecular rovibrational energies. *Spectrochim Acta A Mol Biomol Spectrosc* (2022) 267:120564. doi:10.1016/j.saa.2021.120564

34. Liang DC, Zeng R, Wang CW, Ding QC, Wei LS, Peng XL, et al. Prediction of thermodynamic properties for sulfur dioxide. *J Mol Liq* (2022) 352:118722. doi:10.1016/j.molliq.2022.118722

35. Khordad R, Ghanbari A. Analytical calculations of thermodynamic functions of lithium dimer using modified Tietz and Badawi-Bessis-Bessis potentials. *Comput Theor Chem* (2019) 1155:1–8. doi:10.1016/j.comptc.2019.03.019

36. Ghanbari A, Khordad R. Theoretical prediction of thermodynamic properties of N_2 and CO using pseudo harmonic and Mie-type potentials. *Chem Phys* (2020) 534:110732. doi:10.1016/j.chemphys.2020.110732

37. Khordad R, Ghanbari A. Theoretical prediction of thermodynamic functions of TiC: Morse ring-shaped potential. *J Low Temp Phys* (2020) 199:1198–210. doi:10.1007/s10909-020-02368-8

38. Khordad R, Ghanbari A. Theoretical prediction of thermal properties of K2 diatomic molecule using generalized mobius square potential. *Int J Thermophys* (2021) 42:115. doi:10.1007/s10765-021-02865-2

39. Khordad R, Edet CO, Ikot AN. Application of Morse potential and improved deformed exponential-type potential (IDEP) model to predict thermodynamics properties of diatomic molecules. *Int J Mod Phys C* (2022) 33. doi:10.1142/S0129183122501066

40. Tang B, Jia CS. Relativistic spinless rotation-vibrational energies of carbon monoxide. *Eur Phys J Plus* (2017) 132:375. doi:10.1140/epjp/i2017-11657-7

41. Yanar H, Taş A, Salti M, Aydogdu O. Ro-vibrational energies of CO molecule via improved generalized Pöschl–Teller potential and Pekeris-type approximation. *Eur Phys J Plus* (2020) 135:292. doi:10.1140/epjp/s13360-020-00297-9

42. Eyube EE, Notani PP, Izam MM. Potential parameters and eigen spectra of improved Scarf II potential energy function for diatomic molecules. *Mol Phys* (2022) 120:e1979265. doi:10.1080/00268976.2021.1979265

43. Jia CS, Zhang LH, Peng KL. Improved Pöschl-Teller potential energy model for diatomic molecules. *Int J Quan Chem.* (2017) 117:e25383. doi:10.1002/qua.25383

44. Eyube ES, Notani PP, Dikko AB. Modeling of diatomic molecules with modified hyperbolical-type potential. *Eur Phys J Plus* (2022) 137:329. doi:10.1140/epjp/s13360-022-02526-9

45. Eyube ES, Bitrus BM, Samaila H, Notani PP. Model entropy equation for gaseous substances. *Int J Thermophys* (2022) 43:4355. doi:10.1007/s10765-022-02980-8

46. Eyube ES, Notani PP, Samaila H. Analytical prediction of enthalpy and Gibbs free energy of gaseous molecules. *Chem Thermodynamics Therm Anal* (2022) 6:100060. doi:10.1016/j.ctta.2022.100060

47. Eyube ES, Onate CA, Omugbe E, Nwabueze CM. Theoretical prediction of Gibbs free energy and specific heat capacity of gaseous molecules. *Chem Phys* (2022) 560:111572. doi:10.1016/j.chemphys.2022.111572

48. Eyube ES. Prediction of thermal properties of phosphorus dimer – the analytical approach. *Chem Phys Lett* (2022) 801:139702. doi:10.1016/j.cplett.2022.139702

49. Gordillo-Vázquez FJ, Kunc JA. Statistical–mechanical calculations of thermal properties of diatomic gases. *J Appl Phys* (1998) 84:4693–703. doi:10.1063/1.368712

50. Salinas SRA. *Introduction to statistical physics*. New York: Springer (2001).

51. Strekalov ML. An accurate closed-form expression for the partition function of Morse oscillators. *Chem Phys Lett* (2007) 439:209–12. doi:10.1016/j.cplett.2007.03.052

52. Song XQ, Wang CW, Jia CS. Thermodynamic properties for the sodium dimer. *Chem Phys Lett* (2017) 673:50–5. doi:10.1016/j.cplett.2017.02.010

53. Jia CS, Wang CW, Zhang LH, Peng XL, Zeng R, You XT. Partition function of improved Tietz oscillators. *Chem Phys Lett* (2017) 676:150–3. doi:10.1016/j.cplett.2017.03.068

54. Shi DH, Liu H, Zhang XN, Sun JF, Liu YF, Zhu ZL. MRCI investigations on dissociation energy and molecular constants of BCl ($X\ ^1\Sigma^+$) radical. *Int J Quan Chem.* (2010) 111:2825–34. doi:10.1002/qua.22699

55. Liu X, Truppe S, Meijer G, Pérez-Ríos J. The diatomic molecular spectroscopy database. *J Cheminform* (2020) 12:31. doi:10.1186/s13321-020-00433-8

56. Li R, Zhang X, Feng W, Jiang Y, Fei D, Jin M, et al. *Ab initio* CI calculations on potential energy curves of low-lying states of BrF and its cation including spin–orbit coupling. *Comput Theor Chem* (2014) 1032:20–6. doi:10.1016/j.comptc.2014.01.016

57. Bürger H, Jacob E, Fähnle M. The fourier transform IR spectra of ClF and BrF. *Z Naturforsch* (1986) 41a:1015–20. doi:10.1515/zna-1986-0806

58. Beckert M, Wouters ER, Ashfold MNR, Wrede E. High resolution ion imaging study of BrCl photolysis in the wavelength range 330–570 nm. *J Chem Phys* (2003) 119:9576–89. doi:10.1063/1.1615951

59. Clyne MAA, Curran AH, Coxon JA. Studies of labile molecules with a tunable dye laser: Laser excitation spectrum of BrF ($B\ ^3\Pi\ (0^+) - X\ ^1\Sigma^+$). *J Mol Spectrosc* (1976) 63:43–59. doi:10.1016/0022-2852(67)90133-6

60. National Institute of Standards and Technology (NIST). *NIST chemistry WebBook, NIST standard reference database number 69*. Gaithersburg, Maryland, USA: NIST (2017). doi:10.18434/T42S31